Pramana – J. Phys. (2020) 94:64
https://doi.org/10.1007/s12043-020-1940-y

Features of Jeffrey fluid flow with Hall current: A spectral simulation

V K SINHA[1], B KUMAR[1], G S SETH[1] and R NANDKEOLYAR[2],*

[1]Department of Mathematics & Computing, Indian Institute of Technology (Indian School of Mines), Dhanbad 826 004, India
[2]Department of Mathematics, National Institute of Technology Jamshedpur, Jamshedpur 831 014, India
*Corresponding author. E-mail: rajnandkeolyar@gmail.com

MS received 17 July 2019; revised 2 January 2020; accepted 5 February 2020

Abstract. The Hall current in MHD flow stimulates substantial interest of researchers because of its wide role in many geophysical, astrophysical and fluid engineering situations (construction of turbines, Hall accelerator and centrifugal machines). Motivated by such wide applications, the present work reports the influence of Hall current and thermal radiation on the three-dimensional Jeffrey fluid flow over a stretching surface. In order to achieve similar solution of the governing equations, transformation technique is adopted. The mathematical model is numerically solved by using a spectral technique, namely successive linearisation method (SLM). To explore the feature of various factors, e.g. Hall current and thermal radiation, the variation of flow dominant parameters on the obtained profiles are carefully elucidated with graphs. It can be sensed from the obtained graphs that primary and secondary velocity increase, but, temperature reduces with the enhancement in Hall current. Radiation parameter has the tendency to increase the temperature of the fluid.

Keywords. Hall current; Jeffrey fluid; thermal radiation; successive linearisation method; stretching sheet.

PACS Nos **47.85.ld; 47.65.−d; 47.55.Ca; 47.55.P−**

1. Introduction

The flow of viscous and incompressible fluid due to the continuously moving stretching surface has several uses in many engineering and manufacturing processes. Several types of such models are used in manufacturing long and uniform metal parts, melt spinning technique for cooling liquid, metalworking processes such as hot rolling, rubber sheets, elastic polymer substance, corrosion-resistant fabrics, and production of emollient, paints, glass fibre for thermal insulation etc. Crane [1] was the first to study the steady flow of viscous fluid over a stretching surface and he has found its analytical solution. After Crane [1], many researchers are attracted towards stretching sheet problem and they have started to investigate the flow of fluid having different characteristics. Andersson [2] examined the fluid flow over a stretching surface with two opposite and equal forces acting on the sheet. He has found the analytical solution of the proposed model. The flow of steady, two-dimensional laminar, incompressible and viscous fluid with constant physical properties was studied by Elbashbeshy [3]. Chakrabarti and Gupta [4] have studied fluid flow over a stretching surface in the presence of magnetic and electric fields. They have obtained similar solution. Raptis and Perdikis [5] have examined the influence of chemical reaction on the flow of electrically conducting fluid over a stretching surface and the solutions of the model have been obtained numerically. They have taken such types of fluids in which magnetic Reynolds number is very small. Therefore, applied magnetic field is stronger than the induced magnetic field. Hayat *et al* [6] have investigated the flow of a steady, two-dimensional viscous and third-grade fluid over an exponentially stretching surface in the presence of magnetic field and chemical reaction of first order. They have obtained the analytical solution by using homotopy method. Kumar *et al* [7,8], Ghosh and Mukhopadhyay [9], Ayub *et al* [10] and Mahanthesh *et al* [11] also made contribution on stretching sheet problems.

Investigation on the flow of non-Newtonian fluid has attracted various investigators because of its many uses in scientific, engineering and industrial processes such as aerodynamics, crude oil extraction, thermal and

Published online: 10 April 2020

geothermal insulations. These critical applications are due to the thermophysical properties of non-Newtonian fluids. Especially, heat transfer property of non-Newtonian fluid plays a vital role in polymer industries, manufacturing of petroleum products, food processing etc. It is not possible to represent the physical properties of non-Newtonian fluid by a single equation. Therefore, the physical properties of non-Newtonian fluid are shown by more than one constitutive equations. Regardless of this problem, in recent past, many researchers have studied non-Newtonian fluid flow. Shehzad *et al* [12] investigated the flow of three-dimensional, steady, incompressible Jeffrey fluid over a stretched surface and they have obtained the analytical solution of their problem. A steady Jeffrey fluid flow over a stretching surface is studied by Turkyilmazoglu and Pop [13]. Qasim [14] studied mass and heat transfer of steady two-dimensional Jeffrey fluid flow over a stretching surface. Farooq *et al* [15] investigated the flow of steady two-dimensional Jeffrey fluid in the presence of magnetic field. Hayat *et al* [16] studied Jeffrey fluid stagnation point flow over a stretching surface with Joule heating and viscous dissipation. The flow of Jeffrey fluid under the effect of Cattaneo–Christov heat flux was studied by Hayat *et al* [17]. Rahman *et al* [18] have studied the combined effects of nanoparticles and slip on the flow of incompressible Jeffrey fluid and they have obtained analytical solution. Ahmad and Ishak [19] have examined the flow of Jeffrey fluid in a porous regime over a stretching surface under the effect of magnetic field.

Rate of cooling is very essential for the manufacture of the products. For this purpose, a controlled cooling system is needed. A few years ago, it was difficult to control or regulate the heat for industrial processes. Once the phenomenon of thermal radiation is known, it became very easy to handle the high amount of heat generated in many industrial processes, e.g. nuclear reactors, space vehicles and in manufacturing industrial products. Raptis *et al* [20] have investigated the influence of thermal radiation on the flow of viscous fluid over a stationary plate and obtained the numerical solution. Hayat *et al* [21] studied steady incompressible flow of a second-grade fluid over a fixed plate in the presence of transverse magnetic field and found a series solution. Das *et al* [22] examined the effect of melting heat transfer and thermal radiation on the flow of Jeffrey fluid near the stagnation point in the presence of electric and magnetic fields over a linearly stretched sheet. Kumar *et al* [23,24] have also proposed some fluid flow model with thermal radiation. Mahanthesh *et al* [25] have investigated the hydromagnetic three-dimensional boundary layer flow of nanofluid in the presence of non-linear thermal radiation. Shehzad *et al* [26] have studied the influence of thermal radiation on the flow of three-dimensional steady incompressible MHD Jeffrey fluid over a stretching surface with Brownian motion and thermophoresis. Some other important models based on non-linear thermal radiation are proposed by Mahanthesh *et al* [27,28].

In the presence of magnetic field, conductivity of the ionised gas is affected. Electrons carry electric current in ionised gases. These electrons collide with neutral or charged particles continuously. When the magnetic field is weak, the flow remains axisymmetric but when magnetic field is strong enough to produce Hall current, the flow loses its axisymmetric nature. Sato [29] studied the influence of Hall current on the flow of ionised gas. Three-dimensional steady incompressible MHD fluid flow with Hall current was examined by Katagiri [30]. He has obtained the solution using backward finite differences. Pop and Soundalgekar [31] studied the effect of Hall current on the flow of steady incompressible fluid in the presence of electric and magnetic fields over an infinite porous plate. Reddy [32] has investigated the influence of Joule heating and Hall current on steady two-dimensional MHD convective boundary layer flow over a vertical stretched plate. Gireesha *et al* [33] examined the Hall effect on steady viscous incompressible two-dimensional flow over a non-isothermal surface in the porous regime. They have also considered the effect of thermal radiation and obtained numerical solution of the proposed model. Mahanthesh *et al* [34] recently investigated the effect of nanoparticle shape factor and Hall current on mixed convective flow of nanoliquids. Sreedevi *et al* [35] have studied the effect of Hall current on double diffusive flow of steady incompressible two-dimensional viscous fluid. Shah *et al* [36] examined the impact of Hall current on the flow of steady incompressible micropolar nanofluid in the presence of electric and magnetic fields.

The main aim of this paper is to examine the impact of Hall current and thermal radiation on the flow of three-dimensional incompressible and steady Jeffrey fluid over a stretching sheet in the presence of magnetic field. The model consists of highly non-linear coupled partial differential equations which are not easy to solve analytically. Therefore, we have found similar solution by using successive linearisation method (SLM).

2. Formulation

A steady, three-dimensional and incompressible Jeffrey fluid flow with heat transfer over a stretching surface is considered in the presence of thermal radiation and Hall current. The stretching surface is situated in the xz-plane and it is getting stretched with velocity $u = u_w(x) = ax$ in the x direction. The fluid flow is within the region

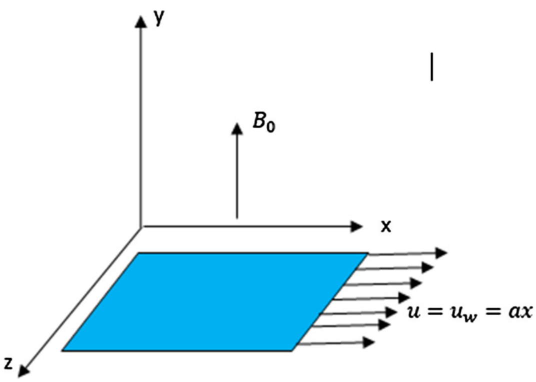

Figure 1. Geometry of the problem.

$y > 0$. A uniform magnetic field of magnitude B_0 acts in a direction normal to the xz-plane. The geometry of the model is displayed in figure 1.

Using these assumptions, the governing equations (continuity, momentum and energy equations) are given below:

$$\frac{\partial u}{\partial x} + \frac{\partial w}{\partial z} + \frac{\partial v}{\partial y} = 0, \tag{1}$$

$$u\frac{\partial u}{\partial x} + w\frac{\partial u}{\partial z} + v\frac{\partial u}{\partial y} = \frac{\nu}{1+\lambda_1}\Big(\frac{\partial^2 u}{\partial y^2} + \lambda_2\Big(\frac{\partial u}{\partial y}\frac{\partial^2 u}{\partial x \partial y} + \frac{\partial v}{\partial y}\frac{\partial^2 u}{\partial y^2} + \frac{\partial w}{\partial y}\frac{\partial^2 u}{\partial z \partial y} + u\frac{\partial^3 u}{\partial x \partial y^2} + v\frac{\partial^3 u}{\partial y^3} + w\frac{\partial^3 u}{\partial z \partial y^2}\Big)\Big) - \frac{\sigma B_0^2}{\rho(1+m^2)}(u+mw), \tag{2}$$

$$u\frac{\partial w}{\partial x} + w\frac{\partial w}{\partial z} + v\frac{\partial w}{\partial y} = \frac{\nu}{1+\lambda_1}\Big(\frac{\partial^2 w}{\partial y^2} + \lambda_2\Big(\frac{\partial u}{\partial y}\frac{\partial^2 w}{\partial x \partial y} + \frac{\partial v}{\partial y}\frac{\partial^2 w}{\partial y^2} + \frac{\partial w}{\partial y}\frac{\partial^2 w}{\partial z \partial y} + u\frac{\partial^3 w}{\partial x \partial y^2} + v\frac{\partial^3 w}{\partial y^3} + w\frac{\partial^3 w}{\partial z \partial y^2}\Big)\Big) + \frac{\sigma B_0^2}{\rho(1+m^2)}(mu-w), \tag{3}$$

$$u\frac{\partial T}{\partial x} + v\frac{\partial T}{\partial y} + w\frac{\partial T}{\partial z} = \frac{\partial}{\partial y}\Big(\Big(\alpha_m + \frac{16\sigma^* T^3}{3\alpha^*\rho c_p}\Big)\frac{\partial T}{\partial y}\Big), \tag{4}$$

where u, w and v are velocity components along the x-axis, z-axis and y-axis respectively. Kinematic viscosity and density of the liquid are represented by ν and ρ respectively. λ_2 and σ are the retardation time and electrical conductivity respectively. λ_1 is the proportion of relaxation to retardation time. m and $\alpha_m = k/\rho c_p$ represent Hall current and liquid's thermal diffusivity. σ^* is the Stefan–Boltzmann constant and α^* is the mean absorption coefficient. Specific heat (pressure constant) is denoted by c_p.

The boundary constraints are

$$\text{At } y=0{:}\ u=u_w=ax;\ v=0;\ w=0;\quad \frac{\partial T}{\partial y} = -h_s T, \tag{5}$$

$$\text{As } y\to\infty{:}\ u'\to 0;\ u\to 0;\ w\to 0;\quad w'\to 0;\ T\to T_\infty. \tag{6}$$

For finding similar solution, the following similarity transformations are used:

$$v = -\sqrt{a\nu}\, f(\eta);\quad u = axf'(\eta);\quad w = axg(\eta), \tag{7}$$

$$\theta(\eta) = \frac{T - T_\infty}{T_\infty};\quad \eta = y\sqrt{\frac{a}{\nu}}. \tag{8}$$

Using these transformations in eqs (2), (3) and (4), we have

$$-(1+\lambda_1)((f')^2 - ff'') + f''' + \beta_1((f'')^2 - ff'''') - \frac{M}{(1+m^2)}(1+\lambda_1)(f'+mg) = 0, \tag{9}$$

$$g'' - (1+\lambda_1)(f'g - fg') + \beta_1(f''g' - fg''') + \frac{M}{(1+m^2)}(1+\lambda_1)(mf'-g) = 0, \tag{10}$$

$$\Big(1 + \frac{4R}{3}(1+\theta)^3\Big)\theta'' + \mathrm{Pr}\, f\theta' + 4R(1+\theta)^2\theta'^2 = 0. \tag{11}$$

The boundary conditions are transformed into

$$\text{At } \eta = 0{:}\ f' = 1;\ g = 0;\ f = 0;\ \theta' = -Bi(1+\theta), \tag{12}$$

$$\text{As } \eta\to\infty{:}\ f'\to 0;\ g\to 0;\ f''\to 0;\ g'\to 0;\ \theta\to 0, \tag{13}$$

where

$$M = \frac{\sigma B_0^2}{\rho a};\quad R = \frac{4\sigma^* T_\infty^3}{k\alpha^*};\quad \mathrm{Pr} = \frac{\nu}{\alpha_m};\quad \beta_1 = \lambda_2 a.$$

Here M is the magnetic parameter, Pr is the Prandtl number, R is the radiation parameter and β_1 is the Deborah number.

There are three most valuable physical quantities which are important for scientific and engineering purposes. These quantities are skin friction coefficients along the x-axis (C_{fx}) and z-axis (C_{fz}) and the local

Nusselt number (Nu_x), which are defined as

$$C_{fx} = \frac{\tau_{wx}}{\rho u_w^2}, \quad C_{fz} = \frac{\tau_{wz}}{\rho u_w^2}, \quad \mathrm{Nu}_x = \frac{x q_w}{k(T - T_\infty)}. \tag{14}$$

Here q_w, τ_{wx} and τ_{wz} are surface heat flux, shear stress of the surface in x-direction, shear stress of the surface (z-direction) respectively. It can be expressed in the following form:

$$\tau_{wx} = \frac{\mu}{1+\lambda_1}\left[\frac{\partial u}{\partial y} + \lambda_2\left(u\frac{\partial^2 u}{\partial x \partial y} + v\frac{\partial^2 u}{\partial y^2}\right)\right]_{y=0},$$
$$\tau_{wz} = \frac{\mu}{1+\lambda_1}\left[\frac{\partial w}{\partial y} + \lambda_2\left(u\frac{\partial^2 w}{\partial x \partial y} + v\frac{\partial^2 w}{\partial y^2}\right)\right]_{y=0}, \tag{15}$$

$$q_w = -k\left(\frac{\partial T}{\partial y}\right) + q_r\Big|_{y=0}, \tag{16}$$

where q_r is the radiative heat flux. Using eqs (15) and (16) in eq. (14), we get

$$C_{fx}\sqrt{\mathrm{Re}_x} = \frac{1}{1+\lambda_1} \times \left[f''(0) + \beta_1\left(f'(0)f''(0) - f(0)f'''(0)\right)\right], \tag{17}$$

$$C_{fx}\sqrt{\mathrm{Re}_x} = \frac{1}{1+\lambda_1} \times \left[g'(0) + \beta_1\left(f'(0)g'(0) - f(0)g''(0)\right)\right], \tag{18}$$

$$\mathrm{Re}_x^{-1/2}\mathrm{Nu}_x = Bi\left[1 + 4R(1+\theta(0))^3\right]\left(1 + \frac{1}{\theta(0)}\right), \tag{19}$$

where $\mathrm{Re}_x = x u_w/\nu$ is the local Reynolds number.

3. Procedure of numerical solution

Similar form of mathematical model, which is presented by eqs (9)–(11) and boundary conditions (12) and (13), is solved by SLM [37,38]. This spectral method follows some assumptions which are given as

(i) The unknown functions $f(\eta)$ $\theta(\eta)$ and $g(\eta)$ are considered as

$$\left.\begin{aligned} f(\eta) &= f_i(\eta) + \sum_{m=0}^{i-1} F_m(\eta), \\ g(\eta) &= g_i(\eta) + \sum_{m=0}^{i-1} G_m(\eta), \\ \theta(\eta) &= \theta_i(\eta) + \sum_{m=0}^{i-1} \Theta_m(\eta), \end{aligned}\right\} \tag{20}$$

where $f(\eta)$, $g(\eta)$ and $\theta(\eta)$ are unknowns and F_m, G_m and Θ_m ($m \geq 1$) are obtained iteratively from the linear part of the equation that are obtained after substitution of (20) into (9)–(11).

(ii) f_i, g_i, θ_i are very small when i tends to a very large number.

The second assumption makes sure that the nonlinear terms in f_i, g_i, θ_i and their derivatives are extremely small. Because of this reason, these terms can be neglected when we substitute eq. (20) in eqs (9)–(11). The initial guesses for F_0, G_0 and Θ_0 are taken as

$$\left.\begin{aligned} &F_0(\eta) = \eta \mathrm{e}^{-\eta}, \qquad G_0(\eta) = \eta \mathrm{e}^{-\eta}, \\ &\Theta_0(\eta) = Bi(\mathrm{e}^{-2\eta}). \end{aligned}\right\} \tag{21}$$

On substituting eq. (20) into eqs (9)–(11), the linearised form of eqs (9)–(11) are as follows:

$$a_{1,i-1}F_i'''' + a_{2,i-1}F_i''' + a_{3,i-1}F_i'' + a_{4,i-1}F_i' + a_{5,i-1}F_i + a_{6,i-1}G_i' = r_{1,i-1}, \tag{22}$$

$$b_{1,i-1}F_i'' + b_{2,i-1}F_i' + b_{3,i-1}F_i + b_{4,i-1}G_i''' + b_{5,i-1}G_i'' + b_{6,i-1}G_i' + b_{7,i-1}G_i = r_{2,i-1}, \tag{23}$$

$$d_{1,i-1}F_i + d_{2,i-1}\Theta_i'' + d_{3,i-1}\Theta_i' + d_{4,i-1}\Theta_i = r_{3,i-1}. \tag{24}$$

The boundary conditions for the linearised scheme are

$$\left.\begin{aligned} &F_i(0) = 0, \quad F_i' = 1, \quad G_i(0) = 0, \\ &\Theta_i'(0) = -Bi(1 + \Theta_i(0)), \\ &F_i'(\infty) = 0, \quad F_i''(\infty) = 0, \quad G_i(\infty) = 0, \\ &G_i'(\infty) = 0, \quad \Theta_i(\infty) = 0. \end{aligned}\right\}$$

The solutions of F_i, G_i and Θ_i, for $i \geq 1$ are calculated recursively by solving eqs (9)–(11), and solutions for $f(\eta)$, $g(\eta)$, $\phi(\eta)$ and $\theta(\eta)$ are written as

$$\left.\begin{aligned} &f(\eta) \approx \sum_{m=0}^{M'} F_m(\eta), \quad g(\eta) \approx \sum_{m=0}^{M'} G_m(\eta), \\ &\theta(\eta) \approx \sum_{m=0}^{M'} \Theta_m(\eta), \end{aligned}\right\}$$

where M' represents the order of approximation. To solve eqs (22)–(24), Chebyshev spectral method is used. In this method, Chebyshev polynomials are particularly defined on [−1 1]. Therefore, we have changed our domain by using the following transformation:

$$\frac{\eta}{L} = \frac{\xi + 1}{2}, \tag{25}$$

where L is the scale parameter.

Table 1. Effect of distinct pertinent flow parameters on Nusselt number and skin-friction.

M	m	R	Pr	$-C_{fx}\,\mathrm{Re}_x^{1/2}$	$C_{fz}\,\mathrm{Re}_x^{1/2}$	$\mathrm{Re}_x^{-1/2}\mathrm{Nu}_x$
1	0.1	0.5	5	1.41126085	0.03915812	1.48725633
2				1.72742011	0.06180346	1.48971803
3				1.99409390	0.07902778	1.49145879
	0.1			1.41126085	0.03915812	1.48725633
	0.3			1.38923473	0.11095147	1.48696434
	0.5			1.35219912	0.16668695	1.48653024
		0.2		1.41126085	0.03915812	2.08151951
		0.3		1.41126085	0.03915812	2.27955722
		0.5		1.41126085	0.03915812	2.47758133
			6	1.41126085	0.03915812	1.48725633
			7	1.41126085	0.03915812	1.48256620
			8	1.41126085	0.03915812	1.47841013

The Gauss–Lobatto collocation points (ξ_i) are taken as

$$\xi_i = \cos\frac{\pi j}{N}, \quad j = 0, 1, 2, \ldots, N. \tag{26}$$

At the collocation points, the functions F_i, G_i and Θ_i are estimated as

$$\left.\begin{aligned} &F_i \approx \sum_{k=0}^{N} F_i(\xi_k)T_k(\xi_j), \quad G_i \approx \sum_{k=0}^{N} G_i(\xi_k)T_k(\xi_j),\\ &\Theta_i \approx \sum_{k=0}^{N} \Theta_i(\xi_k)T_k(\xi_j). \end{aligned}\right\} \tag{27}$$

The kth Chebyshev polynomial (T_k) is calculated as

$$T_k(\xi) = \cos[(\cos^{-1}(\xi))k]. \tag{28}$$

At the collocation points, the rth derivative of the functions F_i, G_i and Θ_i are

$$\left.\begin{aligned} &\frac{\mathrm{d}^r F_i}{\mathrm{d}\eta^r} = \sum_{k=0}^{N} D_{kj}^r F_i(\xi_k), \quad \frac{\mathrm{d}^r G_i}{\mathrm{d}\eta^r} = \sum_{k=0}^{N} D_{kj}^r G_i(\xi_k),\\ &\frac{\mathrm{d}^r \Theta_i}{\mathrm{d}\eta^r} = \sum_{k=0}^{N} D_{kj}^r \Theta_i(\xi_k). \end{aligned}\right\} \tag{29}$$

Here $D = (2/L)\tilde{D}$, $\tilde{D}$ represents Chebyshev spectral differentiation matrix and its elements are defined as

$$\left.\begin{aligned} &\tilde{D}_{jk} = \frac{c_j(-1)^{j+k}}{c_k\xi_j - \xi_k}, \quad j \neq k;\ j,\ k = 0, 1, \ldots, N,\\ &\tilde{D}_{kk} = -\frac{\xi_k}{2(1-\xi_k^2)}, \quad k = 1, 2, \ldots, N-1,\\ &\tilde{D}_{00} = \frac{2N^2+1}{6}, \ \tilde{D}_{NN} = -\frac{2N^2+1}{6}. \end{aligned}\right\}$$

Substituting (25)–(29) into (22)–(24), we have obtained the following matrix equation:

$$A_{i-1}X_i = R_{i-1},$$

where A_{i-1} is a square matrix of order $(2N+2)*(2N+2)$ and X_i and R_{i-1} are column vectors of order $(2N+2)*1$. Finally, the solution is defined by

$$X_i = A_{i-1}^{-1} * R_{i-1}.$$

4. Results

In this paper, steady three-dimensional MHD Jeffrey fluid flow over a stretching surface is investigated with Hall current and thermal radiation. In this section, the impact of distinct parameters M, m, R and Pr on the flow field and temperature field is discussed. In addition to it, table 1 containing the values of skin friction (x- and z-directions) and local Nusselt number with disparate flow domination parameters, is presented. For the complete analysis, we have taken $M = 1$, $m = 0.1$, $R = 0.2$, Pr$=$ 6, $\lambda_1 = 0.1$, $\beta_1 = 0.1$ and $Bi = 0.1$, as default values [25,33] of parameters. However, the changes made in the values of particular parameters [39] are shown in respective figures and table.

The impacts of magnetic parameter (M) on the flow field and temperature field are displayed in figures 2 – 4. As we know, in the presence of magnetic parameter, a magnetic field is induced which produces a resistive force. It is known as Lorentz force. Nature of the Lorentz force is to oppose the fluid motion, and due to this, primary velocity (velocity along the x-direction) shows opposite trend with magnetic parameter. As M enhances, the velocity along the z direction (secondary velocity) increases near the sheet but away from it, secondary velocity reduces. But on other hand, temperature profiles rise with the enhancement in M.

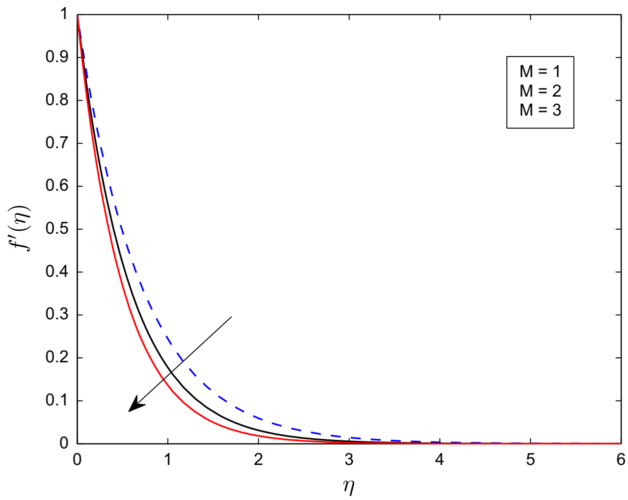

Figure 2. Primary velocity distribution for M.

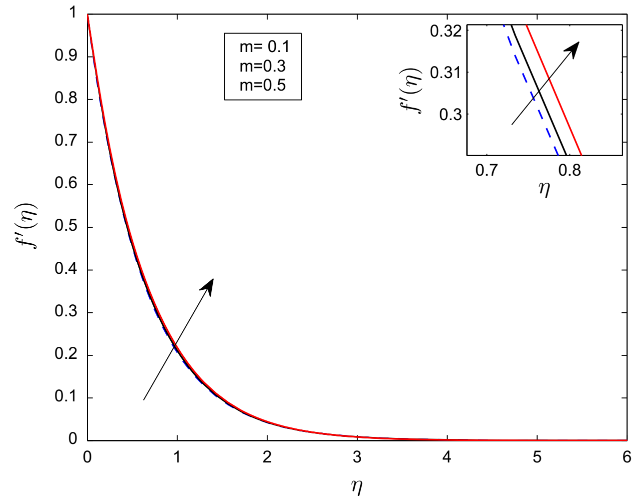

Figure 5. Primary velocity distribution for m.

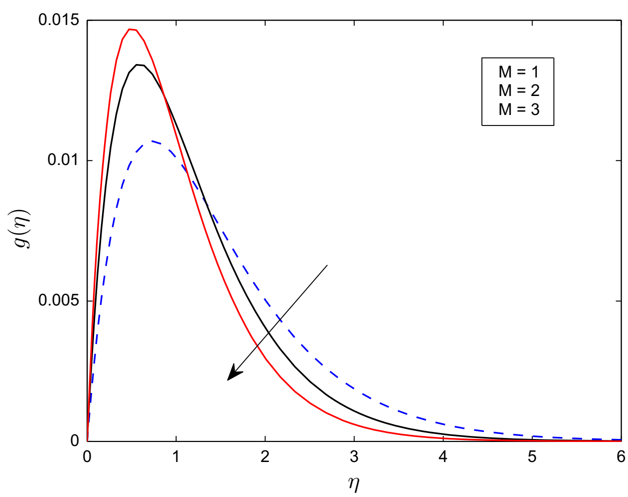

Figure 3. Secondary velocity distribution for M.

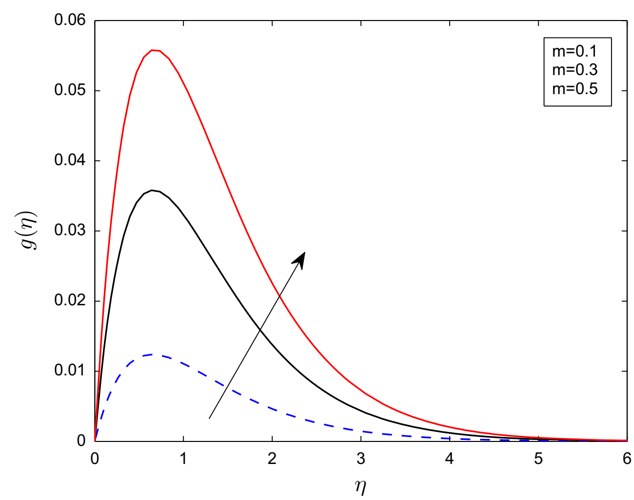

Figure 6. Secondary velocity distribution for m.

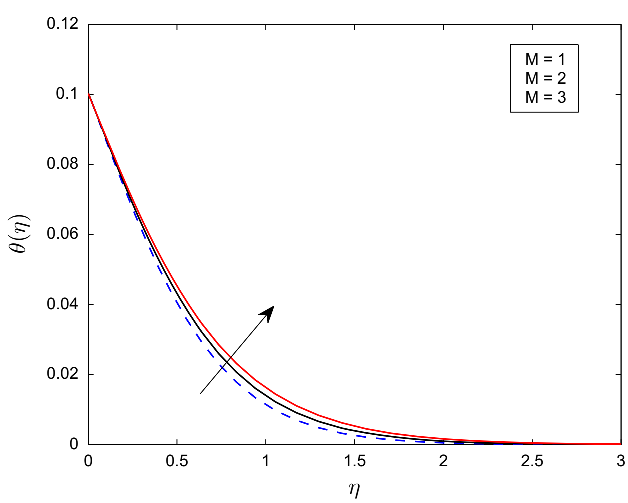

Figure 4. Temperature distribution for M.

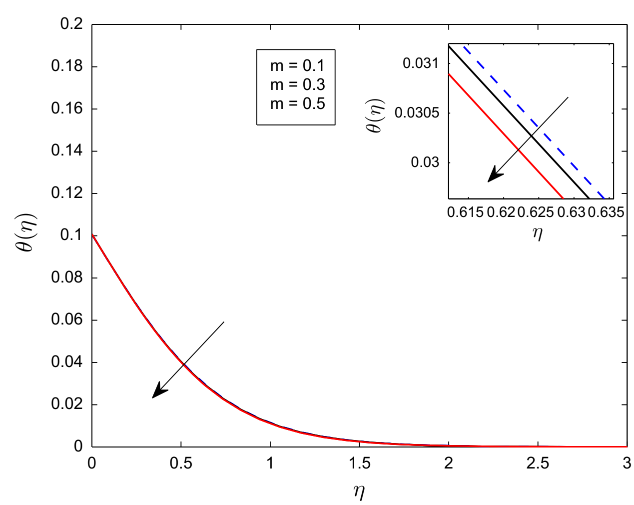

Figure 7. Temperature distribution for m.

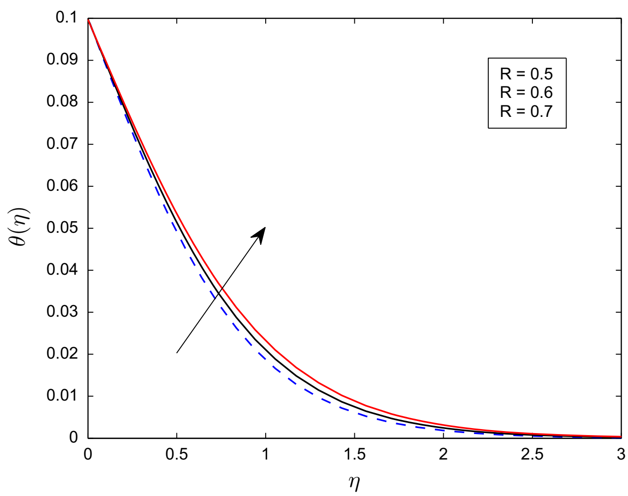

Figure 8. Temperature distribution for R.

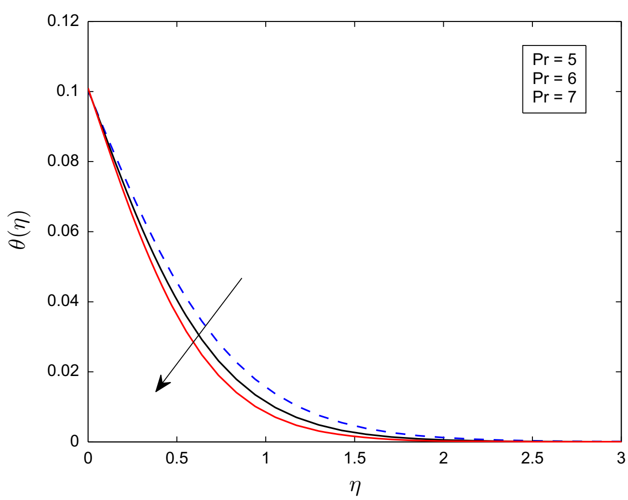

Figure 9. Temperature distribution for Pr.

Hall current parameter (m) estimates the impact of Hall current on different physical behaviours of the fluid. The effects of m on velocities (primary and secondary) are depicted in figures 5 and 6. Both velocities increase with increment in m. As larger value of m decreases the effective conductivity of the fluid, decrement in magnetic damping force is found and hence velocity increases in the x- and z-directions. From figure 7, it can be noticed that temperature field shows opposite trend due to parameter m.

The impacts of thermal radiation (R) and Prandtl number (Pr) on temperature distribution are displayed in figures 8 and 9 respectively. From figure 8, it is clear that the temperature of the fluid rises with enhancement in R. Generally, it is noted that more heat is absorbed by the fluid in the presence of thermal radiation and so, due to temperature gradient, diffusion flux occurs. Therefore, increment in fluid temperature can be noticed with the increment in R. However, temperature field gets retarded with increasing values of Pr. Prandtl number is defined as the proportion of momentum diffusivity to thermal diffusivity. As Pr increases, the thermal diffusivity decreases and hence it decreases the energy transfer ability. Effectively, a decrement in temperature profiles is noticed as we increase the value of Pr.

The effects of distinct pertinent parameters M, m, R and Pr on skin friction coefficients (z- and x-directions) and local Nusselt number are shown in table 1. Rate of heat transfer starts to increase with increment in M and R. However, it decreases with increment in m and Pr. Magnetic parameter M enhances skin friction coefficients in both directions, i.e. x and z, because magnetic field induces a resistive force in the fluid flow, the force opposes the fluid motion and therefore, greater shear stress within the boundary layer is noticed. The parameter m has a tendency to enhance skin friction along the x-direction and reduce it along the z-direction.

5. Conclusions

This is a significant investigation for Jeffrey fluid flow with Hall current and thermal radiation. The most important findings of our investigation are summarised below:

(i) Magnetic parameter M reduces the momentum boundary layer thickness in x- and z-directions. Due to magnetic parameter, enhancement in shear stress in both directions has occurred.

(ii) The secondary fluid velocity enhances near the surface and then reduces away from the surface with increment in M. The skin friction coefficient along z-axis increases due to M.

(iii) The velocities (z- and x-directions) and skin friction coefficient in z-axis enhance with increment in m. However, temperature profile and skin friction coefficient along the x-axis reduce due to Hall current.

(iv) Thermal radiation has a tendency to enhance temperature. However, Pr diminishes the temperature profile.

(v) Nu_x increases with increment in M and R, but it reduces with increment in m and Pr.

Acknowledgements

One of the authors, R Nandkeolyar, thankfully acknowledges the grant received from Science and Engineering Research Board, Department of Science and Technology, Government of India (File No.: ECR/2017/000118/PMS).

References

[1] L J Crane, *Z. Angew. Math. Physik* **21**, 645 (1970)
[2] H Andersson, *Acta Mech.* **95**, 227 (1992)
[3] E M Elbashbeshy, *J. Phys. D* **31**, 1951 (1951)
[4] A Chakrabarti and A Gupta, *Quart. Appl. Math.* **37**, 73 (1979)
[5] A Raptis and C Perdikis, *Int. J. Non-Linear Mech.* **41**, 527 (2006)
[6] T Hayat, M I Khan, M Waqas, A Alsaedi and T Yasmeen, *Chin. J. Chem. Eng.* **25**, 257 (2017)
[7] B Kumar, G S Seth and R Nandkeolyar, *Pramana – J. Phys.* **93**: 74 (2019)
[8] B Kumar, G S Seth and R Nandkeolyar, *Proc. Inst. Mech. Eng. E*, https://doi.org/10.1177/0954408919878984 (2019)
[9] S Ghosh and S Mukhopadhyay, *Pramana – J. Phys.* **92**: 93 (2019)
[10] K Ayub, M Y Khan, Q M Ul-Hassan, M Ashraf and M Shakeel, *Pramana – J. Phys.* **91**: 83 (2018)
[11] B Mahanthesh, I L Animasaun, M Rahimi-Gorji and I M Alarifi, *Physica A* **535**, 122471 (2019)
[12] S Shehzad, A Alsaedi and T Hayat, *Int. J. Heat Mass Transf.* **55**, 3971 (2012)
[13] M Turkyilmazoglu and I Pop, *Int. J. Heat Mass Transf.* **57**, 82 (2013)
[14] M Qasim, *Alex. Eng. J.* **52**, 571 (2013)
[15] M Farooq, N Gull, A Alsaedi and T Hayat, *J. Mech.* **31**, 319 (2015)
[16] T Hayat, M Waqas, S A Shehzad and A Alsaedi, *J. Hydrol. Hydromech.* **63**, 311 (2015)
[17] T Hayat, S Qayyum, M Imtiaz and A Alsaedi, *PLOS One*, **11**, e0148662 (2016)
[18] S Rahman, R Ellahi, S Nadeem and Q M Z Zia, *J. Mol. Liq.* **218**, 484 (2016)
[19] K Ahmad and A Ishak, *Propuls. Power Res.* **6**, 269 (2017)
[20] A Raptis, C Perdikis and H S Takhar, *Appl. Math. Comput.* **153**, 645 (2004)
[21] T Hayat, Z Abbas, M Sajid and S Asghar, *Int. J. Heat Mass Transf.* **50**, 931 (2007)
[22] K Das, N Acharya and P K Kundu, *Alex. Eng. J.* **54**, 815 (2015)
[23] B Kumar, G S Seth and R Nandkeolyar, *Phys. Scr.* **94**, 115211 (2019)
[24] B Kumar, G S Seth and R Nandkeolyar, *Int. J. Therm. Sci.* **146**, 106101 (2019)
[25] B Mahanthesh, B J Gireesha and R S Gorla, *J. Nigerian Math. Soc.* **35**, 178 (2016)
[26] S Shehzad, Z Abdullah, A Alsaedi, F Abbasi and T Hayat, *J. Magn. Magn. Mater.* **397**, 108 (2016)
[27] B Mahanthesh, B J Gireesha, S A Shehzad, A Rauf and P S Kumar, *Physica B* **537**, 98 (2018)
[28] B Mahanthesh, B J Gireesha and I L Animasaun, *J. Nanofluids* **7**, 833 (2018)
[29] H Sato, *J. Phys. Soc. Jpn.* **16**, 1427 (1961)
[30] M Katagiri, *J. Phys. Soc. Jpn.* **27**, 1051 (1969)
[31] I Pop and V Soundalgekar, *Acta Mech.* **20**, 315 (1974)
[32] M G Reddy, *Ain Shams Eng. J.* **5**, 169 (2014)
[33] B J Gireesha, B Mahanthesh, R S R Gorla and P T Manjunatha, *Heat Mass Transf.* **52**, 897 (2016)
[34] B Mahanthesh and I L Animasaun, *Multidiscip. Model. Mater. Struct.* **15**, 758 (2019)
[35] G Sreedevi, R R Rao, D P Rao and A Chamkha, *Ain Shams Eng. J.* **7**, 383 (2016)
[36] Z Shah, S Islam, T Gul, E Bonyah and M A Khan, *Results Phys.* **9**, 1201 (2018)
[37] Z Makukula, P Sibanda and S Motsa, *Bound. Value Probl.* **2010**, 471793 (2010)
[38] S S Motsa and P Sibanda, *Comput. Math. Appl.* **63**, 1197 (2012).
[39] S A Shehzad, T Hayat, M S Alhuthali and S Asghar, *J Cent. South Univ.* **21**, 1428 (2014)